

SPE/DOE 24195

## Reduction of Oil and Water Permeabilities Using Gels

J. Liang, H. Sun, and R.S. Seright, New Mexico Petroleum Recovery Research Center

SPE Members

Copyright 1992, Society of Petroleum Engineers Inc.

This paper was prepared for presentation at the SPE/DOE Eighth Symposium on Enhanced Oil Recovery held in Tulsa, Oklahoma, April 22-24, 1992.

This paper was selected for presentation by an SPE Program Committee following review of information contained in an abstract submitted by the author(s). Contents of the paper, as presented, have not been reviewed by the Society of Petroleum Engineers and are subject to correction by the author(s). The material, as presented, does not necessarily reflect any position of the Society of Petroleum Engineers, its officers, or members. Papers presented at SPE meetings are subject to publication review by Editorial Committees of the Society of Petroleum Engineers. Permission to copy is restricted to an abstract of not more than 300 words. Illustrations may not be copied. The abstract should contain conspicuous acknowledgment of where and by whom the paper is presented. Write Librarian Manager, SPE, P.O. Box 833836, Richardson, TX 75083-3836. Telex, 730639 SPEDAL.

### Abstract

Several previous researchers reported that polymers or gels can reduce permeability to water more than to oil. However, a plausible explanation for the phenomenon is not yet available. This property is critical to the success of gel treatments in production wells if zones cannot be isolated during gel placement. We examined how different types of gels reduce oil and water permeabilities in Berea sandstone. The gel formulations that we investigated included (1) resorcinol-formaldehyde, (2)  $\text{Cr}^{3+}$ (chloride)-xanthan, (3)  $\text{Cr}^{3+}$ (acetate)-polyacrylamide, and (4) colloidal silica. Several new methods were applied to obtain a better understanding of why gels can reduce water permeability more than oil permeability. First, before gel placement in cores, multiple imbibition and drainage cycles were performed in both flow directions. Results from these studies established that hysteresis of oil and water relative permeabilities was not responsible for the behavior observed during our subsequent gel studies. Second, several gels clearly reduced water permeability significantly more than oil permeability. Whereas previous literature reported this phenomenon for polymers and "weak" polymer-based gels, we also observed the disproportionate permeability reduction with a monomer-based gel (resorcinol-formaldehyde), as well as with both "weak"  $\text{Cr}^{3+}$ (chloride)-xanthan and "strong"  $\text{Cr}^{3+}$ (acetate)-HPAM gels. In contrast, a colloidal-silica gel reduced water and oil permeabilities by about the same factor. Residual resistance factors for several gels were found to erode during multiple cycles of oil and water injection. In spite of this erosion, the disproportionate permeability reduction persisted through the cycles for most of the gels. Studies using both oil and water tracers provided insight into the fraction of the pore volume occupied by gel. The strongest gels appeared to encapsulate the original residual oil saturation—thus rendering the residual oil inaccessible during subsequent oil flooding.

References and figures at end of paper.

### Introduction

Applications of near-wellbore gel treatments in production wells are intended to reduce excess water production without sacrificing oil production. In a previous study,<sup>1</sup> we developed a theoretical model using fractional flow and material balance concepts to quantify the degree of gelant penetration into oil-productive zones, as well as into water-source zones. (The term "gelant" here refers to the liquid formulation prior to gelation.) The study showed that gelants can penetrate to a significant degree into all open zones—not just those zones with high water saturations. The study also indicated that oil productivity can be impaired even if the gel reduces water permeability without affecting oil permeability. The principal advantage of the disproportionate reduction of the water and oil relative permeabilities is in reducing the need for zone isolation during gel placement. Realizing this advantage generally requires high fractional oil flow from the zone(s) of interest. During the study, the effects of capillary pressure were neglected in order to obtain a closed-form solution to the water conservation equation.

In a separate study,<sup>2</sup> we examined the effects of capillary pressure on gel placement. This study showed that, in coreflood experiments in oil-wet cores, capillary effects could inhibit an aqueous gelant from entering a core. However, in field applications, the pressure drop between injection and production wells is usually so large that capillary effects will not prevent gelant penetration into oil-productive zones. Under field-scale conditions, the effects of capillary pressure on gelant fractional flow are negligible. Hence, capillary pressure effects do not change the conclusions reached in Ref. 1, where capillary effects were neglected.

Several researchers<sup>3-10</sup> reported that some polymers and gels can reduce permeability to water more than to oil. Fig. 1 provides a summary of the results from different researchers. In this figure, the permeability reduction for water at residual

oil saturation is plotted against the permeability reduction for oil at residual water saturation. A given permeability-reduction value was determined by dividing the end-point permeability before exposure to polymer or gel by the end-point permeability after exposure to polymer or gel. Using this definition, two factors contributed to the permeability reductions—(1) changes in permeability at a given fluid saturation and (2) changes in end-point fluid saturations. The available evidence indicates that polymer or gel usually shifted the entire water relative permeability curve to lower values without significantly changing the residual oil saturation. In contrast, the position of the oil relative permeability curve was often unaffected by the polymer or gel, except that the irreducible water saturation was increased. Thus, the increase in the irreducible water saturation was largely responsible for permeability reductions for oil.

The disproportionate permeability reduction is critical to the success of gel treatments in production wells if zones cannot be isolated during gel placement.<sup>1</sup> The ultimate objectives of our research in this area are to determine the reason why the disproportionate permeability reduction occurs and to identify conditions that maximize this phenomenon.

In this study, we examined how different types of gels reduce oil and water permeabilities in Berea sandstone. The impact of wettability on reduction of oil and water permeabilities was investigated. We also examined whether hysteresis of end-point oil and water permeabilities occurs during the "pump-in, pump-out" sequence used during gel treatments.

### Experimental Procedures

**Gelants Studied.** Four types of gels were investigated in this study, including: (1) resorcinol-formaldehyde, (2) Cr<sup>3+</sup>(chloride)-xanthan, (3) Cr<sup>3+</sup>(acetate)-polyacrylamide (Marathon's MARCIT<sup>®</sup>), and (4) colloidal silica (DuPont's Ludox SM<sup>®</sup>). For the Cr<sup>3+</sup>(acetate)-polyacrylamide gel, three formulations of different final strength were used. Table 1 lists the compositions of these gelants. Pfizer provided the xanthan (Flocon 4800<sup>®</sup>), DuPont supplied the colloidal silica, and Marathon provided the polyacrylamide. The polyacrylamide (HPAM) had a molecular weight of about 2 million daltons and a degree of hydrolysis of 2 percent. The other chemicals used in this study were reagent grade.

**Coreflood Procedures.** The sequence followed during our core experiments is summarized in Table 2. All experiments were conducted at 41°C. Berea sandstone cores were used that had a nominal absolute permeability to brine of 800 md. All cores were about 15 cm long and 3.6 cm in diameter. All cores had one internal pressure tap located 2.5 cm from the inlet rock face. The cores were not fired.

Water-tracer studies were performed after the core was first saturated with brine and after each waterflood. These studies involved injecting a brine bank that contained 40-ppm potassium iodide as a tracer. The tracer concentration in the effluent was monitored spectrophotometrically at a wavelength of 230 nm. For our latest experiments, oil-tracer studies were

performed after each oilflood. These studies involved injecting an oil bank that contained 20-ppm trans-stilbene as a tracer. The tracer concentration in the effluent was monitored spectrophotometrically at a wavelength of 300 nm. Usually, four replicates were performed for each tracer study. Also, the replicates included studies performed at different injection rates. Retention of trans-stilbene in Berea sandstone was found to be negligible (less than 0.01 µg/g of rock).

**Hysteresis Studies Before Gel Placement.** The relative permeability of a given phase is often both path- and history-dependent.<sup>11,12</sup> Gel treatments in production wells involve a "pump-in, pump-out" sequence where an aqueous gelant is injected into a production well from one direction, and later, oil is produced from the opposite direction. Hysteresis of relative permeability curves can result in significant damage to oil productivity.<sup>1</sup> Thus, the impact of this hysteresis should be considered prior to a gel treatment. Our coreflood experiments were designed to examine the effects of flow-direction reversal and multiple imbibition and drainage cycles on end-point oil and water relative permeabilities at irreducible water and oil saturations, respectively.

Both a crude oil from West Texas (Moutray) and a refined oil (Soltrol-130<sup>®</sup>) were used in our studies. To achieve an intermediate wettability,<sup>13-15</sup> cores were aged with Moutray crude oil at 80°C for eight days after the first oilflood (Step 4 in Table 2). Then, the old crude oil was displaced by three pore volumes (PV) of fresh crude oil and the oil mobility was determined. Tests revealed that the Amott indexes for oil and water were both near zero—indicating intermediate wettability. When the refined oil was used in place of the crude oil, cores were strongly water-wet.

In each of the corefloods, Steps 1 through 10 (outlined in Table 2) were performed to characterize the core and to establish baselines before gelant injection. Table 3 provides a summary of the hysteresis studies before gelant injection. The results were reproducible during replicate cycles. For the strongly water-wet cores (i.e., the cores with the refined oil), no significant hysteresis of end-point permeabilities (either for water or oil) was observed as a result of the flow-direction reversal. However, for the cores with intermediate wettability (i.e., the cores with the crude oil), flow-direction reversal caused a 45 to 73% increase in end-point permeability to water. A much smaller hysteresis was observed for end-point oil permeability. More detailed results from our hysteresis studies can be found in Ref. 16.

The main value of these studies is that they quantify the importance of hysteresis in our fluid/rock systems prior to the introduction of gel. Especially for those parameters that were unaffected by flow-reversal and multiple imbibition and drainage cycles, gel effects can now be distinguished from hysteresis effects during our subsequent gel studies.

**Gelant Placement Procedures.** For the resorcinol-formaldehyde gelant, retention studies in Berea sandstone cores revealed no significant loss of gelant components, either by adsorption or by partitioning into the oil phase. Therefore, only 3 PV of the gelant were injected. This gelant was water-like during the injection process (Step 11). In contrast, 10 PV

of  $\text{Cr}^{3+}$  (chloride)-xanthan gelant were injected to ensure that the cores were saturated with the gelant. For the  $\text{Cr}^{3+}$  (acetate)-HPAM gelant with 1.39% HPAM and 636-ppm  $\text{Cr}^{3+}$ , approximately 4 PV of gelant were injected because a high pressure gradient developed. For the  $\text{Cr}^{3+}$  (acetate)-HPAM gelant with 1.35% HPAM and 212-ppm  $\text{Cr}^{3+}$ , 8 PV of gelant was injected before the pressure gradient reached the pressure constraint. For the  $\text{Cr}^{3+}$  (acetate)-HPAM gelant with 0.7% HPAM and 318-ppm  $\text{Cr}^{3+}$ , 10 PV were injected. Ten PV of gelant were also injected during the experiments with colloidal silica.

We examined how the presence of oil affects gelation. During tests in bottles, both the refined oil and Moutray crude had no effect on the gelation times or the appearance of the gels. Also, during all of the core experiments, injected and non-injected gelant formulations exhibited similar gelation times and final gel strengths. The shut-in times (five days) were 8 to 33 times longer than the gelation times. (Detailed gel placement data can be found in Ref. 16.)

Effluent samples were collected throughout the process of injecting the  $\text{Cr}^{3+}$  (chloride)-xanthan and  $\text{Cr}^{3+}$  (acetate)-HPAM gelants. These samples were analyzed for chromium concentration using atomic absorption spectrometry. The results for  $\text{Cr}^{3+}$  (chloride)-xanthan gelant are presented in Fig. 2. A case with no residual oil<sup>17</sup> is included for comparison with the two cases where residual oil was present. For the case without residual oil, the first chromium in the effluent was detected after injecting 3 PV of gelant. After injecting 10 PV, the chromium concentration in the effluent reached about 80% of its injected value. Fig. 2 indicates that chromium propagates more readily in porous media with residual oil present. For the cases with residual oil present, the first chromium in the effluent was detected after injecting 1 PV of gelant. The chromium concentration in the effluent then increased steadily and leveled off at over 90% of the injected concentration. The more rapid breakthrough of chromium when oil is present occurs partly because residual oil decreases the pore volume occupied by water. However, this explanation does not entirely account for the different  $\text{Cr}^{3+}$  propagation rates with versus without residual oil. Additional chromium propagation data for  $\text{Cr}^{3+}$  (chloride)-xanthan gelants and for the  $\text{Cr}^{3+}$  (acetate)-HPAM gelants are documented in Ref. 16.

#### Permeability Reduction for Oil and Water After Gel Treatment

Following the five-day shut-in period, Steps 13 through 17 (from Table 2) were performed to determine the residual resistance factors for brine ( $F_{rw}$ ) and oil ( $F_{ro}$ ). (See the Nomenclature for definitions of these terms.) In order to simulate the "pump-in, pump-out" sequence used during gel treatments in production wells, the gelant was injected into the core from one direction (flow direction #1), and residual resistance factors were measured in the opposite direction (flow direction #2). The hysteresis effects, if present, were eliminated by using the end-point mobilities measured in the same direction (flow direction #2) before and after gel treatments to calculate residual resistance factors. Results are

summarized in Table 4. More detailed results can be found in Ref. 16.

**Resorcinol-Formaldehyde.** For the resorcinol-formaldehyde gel in both the water-wet and intermediate-wet systems, residual resistance factors were more or less Newtonian (velocity independent) during continuous injection of either water or oil. (We also noted Newtonian behavior during water injection in a previous study where no oil was present.<sup>18</sup>) However, the  $F_{rw}$  value during the second waterflood (Step 15c) was less than the previous  $F_{rw}$  value (Step 13). This suggests that the gel experienced physical breakdown during the oil-water injection cycle. Further gel breakdown was not observed during a subsequent oil-water injection cycle (Steps 16a through 16d).

**$\text{Cr}^{3+}$  (Chloride)-Xanthan.** The  $F_{rw}$  and  $F_{ro}$  values for the  $\text{Cr}^{3+}$  (chloride)-xanthan gels were generally lower than those for the other gels. The  $F_{rw}$  values were also much lower than those measured in our previous studies without a residual oil saturation.<sup>17,19</sup> Gel breakdown was not observed during the oil-water injection cycles. The flow-rate dependence of  $F_{rw}$  values was very weak for the data with residual oil present. In contrast, a strong apparent shear-thinning behavior was observed during other studies, where residual oil was not present.<sup>17,19</sup> Further work will be needed to understand the reasons for these differences.

For both the resorcinol-formaldehyde gel and the  $\text{Cr}^{3+}$  (chloride)-xanthan gel, the  $F_{rw}$  and  $F_{ro}$  values were lower for the strongly water-wet cores than for the intermediate-wet cores (see Table 4). Thus, these gels reduced oil and water permeabilities to a greater extent in the intermediate-wet cores than in the strongly water-wet systems. For the  $\text{Cr}^{3+}$  (chloride)-xanthan gel, the impact of wettability on the ratio,  $F_{rw}/F_{ro}$ , was not significant. However, for the resorcinol-formaldehyde gel, the disproportionate permeability reduction was more pronounced for the system of intermediate wettability than for the strongly water-wet system. A high  $F_{rw}/F_{ro}$  ratio is beneficial in reducing the need for zone isolation during gel placement in production wells.<sup>1</sup> Of course,  $F_{ro}$  values greater than one will reduce oil productivity to some extent.

**$\text{Cr}^{3+}$  (Acetate)-HPAM.** Three  $\text{Cr}^{3+}$  (acetate)-HPAM formulations were examined in this study. In all cases, the flow of brine in the porous medium exhibited a strong apparent "shear-thinning" behavior, while the flow of oil remained Newtonian. As indicated in Table 4, the relationship between  $F_{rw}$  and superficial velocity,  $u$ , could be described using a power-law equation. In some cases, because the residual resistance factors for water were so high, experiments could only be performed at a single, low injection rate. Thus, we were not able to determine, in these cases, how  $F_{rw}$  varied with injection rate. For all the  $\text{Cr}^{3+}$  (acetate)-HPAM formulations, both  $F_{rw}$  and  $F_{ro}$  values were reduced during the subsequent oil-water injection cycles (Table 4).

The largest ratios of  $F_{rw}$  to  $F_{ro}$  were observed for the  $\text{Cr}^{3+}$  (acetate)-HPAM gels. For example, the  $\text{Cr}^{3+}$  (acetate)-HPAM gel with 1.39% HPAM and 212-ppm  $\text{Cr}^{3+}$  provided an extremely high  $F_{rw}$  value (53,000) during brine injection

immediately after shut-in. During the following oil-water injection cycle, the residual resistance factor for oil (Soltrol-130) was 50, and the residual resistance factor for water could be described by a power-law equation,  $F_{rrw} = 972 u^{-0.70}$ . After two additional oil-water injection cycles, the  $F_{rro}$  value stabilized at 14. At the end, the  $F_{rrw}$  values could be described by a power-law equation,  $F_{rrw} = 105 u^{-0.55}$ . For the same  $Cr^{3+}$  (acetate)-HPAM formulation, similar behavior was reported in previous water- $CO_2$  experiments.<sup>2</sup>

**Colloidal Silica.** For the colloidal-silica gel, continuous gel breakdown was observed during the first brine injection after shut-in. The first  $F_{rrw}$  value measured immediately after shut-in at a superficial velocity of 0.023 ft/d was about 3,200. The  $F_{rrw}$  values then decreased with increased flow-velocity and eventually stabilized at about 26. Table 4 shows that further gel breakdown occurred during the subsequent oil-water injection cycles. During these experiments, the pressure gradient never exceeded 200 psi/ft. In contrast, in earlier work, Jurinak *et al.*<sup>20</sup> found that pressure gradients above 2500 psi/ft were required to cause gel breakdown. Additional work is needed to explain this finding. The flow behavior for the refined oil or brine in the porous medium was Newtonian.

Table 4 shows that, except for the colloidal-silica gel, all other gels tested in this study reduced water permeability more than oil permeability ( $F_{rrw} > F_{rro}$ ). For the colloidal-silica gel,  $F_{rrw}$  and  $F_{rro}$  values were about the same during a given oil-water cycle.

### Results from Tracer Studies

Tracer studies were performed to determine pore volumes and dispersivities of the cores. Traditional error-function solutions<sup>21</sup> did not fit the tracer curves well during water injection when residual oil was present. In particular, the tracer curves were asymmetric. Therefore, volume balances were required to determine the fraction of the pore volume that remained open to flow.

We did not develop the oil-tracer procedure until after completing the studies of the resorcinol-formaldehyde and  $Cr^{3+}$  (chloride)-xanthan gels. Therefore, results from oil-tracer studies are only available for the  $Cr^{3+}$  (acetate)-HPAM and the colloidal-silica gels. Results from our tracer studies are summarized in Tables 5 through 10 and in Figs. 3 and 4. The ratio,  $V_p/V_{po}$ , represents the fraction of the original pore volume that was sampled by the tracer during a given tracer study. The difference,  $1 - V_p/V_{po}$ , represents the fraction of the original pore volume that was occupied by the immobile phase and/or gel. The quantity,  $\alpha$ , shown in Figs. 3 and 4 refers to the dispersivity during a given tracer study. The  $\alpha$  values were obtained using a mixing zone that extends from 10% to 90% of the injected tracer concentration.<sup>21</sup>

The first parts of Tables 5 through 10 show that prior to gel placement,  $S_{or}$  and  $S_{wr}$  values obtained from water- and oil-tracer studies usually agreed well with those from volumetric measurements. The results of pore volume determinations from both oil- and water-tracer studies were reproducible during replicate cycles.<sup>16</sup>

**Resorcinol-Formaldehyde.** For the resorcinol-formaldehyde gel in a strongly water-wet core (Table 5), the water-tracer studies indicate that gel plus oil occupied 37% of the original pore volume immediately after the gel treatment. A comparison of this number with the residual oil saturation ( $S_{or} = 0.34$ ) indicates that the gel occupied only 3% of the original pore volume. Because this gel provided significant permeability reductions ( $F_{rrw} = 40$  to 49), the small quantity of gel may occupy strategic locations in pore throats.

**$Cr^{3+}$  (Chloride)-Xanthan.** For the  $Cr^{3+}$  (chloride)-xanthan gel in a strongly water-wet core (Table 6), a comparison of the water-tracer results and the  $S_{or}$  value indicates that the gel occupied 28% of the original pore volume (61% minus 33%). However, results from the subsequent water-tracer study show an increase from 61% to 80% for the pore volume occupied by the gel plus oil. Since no more gelant was injected during the process, this increase can only be attributed to an increase in residual oil saturation. Thus, the gel appears to trap additional oil during the latter oil-water injection cycles. This phenomenon was also observed with the resorcinol-formaldehyde gel (Table 5). The phenomenon was not observed for the case with  $Cr^{3+}$  (chloride)-xanthan gel in a core with intermediate wettability.<sup>16</sup> Additional work is needed to explain this phenomenon.

**$Cr^{3+}$  (Acetate)-HPAM.** For the  $Cr^{3+}$  (acetate)-HPAM gel with 1.39% HPAM and 212-ppm  $Cr^{3+}$ , extremely high residual resistance factors for water precluded water-tracer studies during the first oil-water injection cycle. However, water- and oil-tracer studies were performed throughout the rest of the study. The pore volume determinations from water- and oil-tracer studies are summarized in Tables 7 and 8, respectively. Material balance calculations (Table 7) show an increase in residual oil saturation during the first oil-water injection cycle after gelation (from 29% to 34%). The water-tracer studies and the material balance calculations (last row of Table 7) indicate that gel occupied 51% of the original pore volume after three oil-water injection cycles (84% minus 33%).

The last row in Table 8 shows that the oil tracer sampled only 20% of the original pore volume. However, material balance calculations indicate that gel plus trapped water occupied about 55% of the original pore volume. This means that about 25% of the original pore volume was occupied by immobile oil. This value is near the residual oil saturation before gel treatment (Table 7). Thus, the gel appears to have encapsulated the original residual oil saturation and rendered it immobile during subsequent oil floods. Similar results were observed for the  $Cr^{3+}$  (acetate)-HPAM gel with 1.39% HPAM and 636-ppm  $Cr^{3+}$ .<sup>16</sup>

Comparing the last  $V_p/V_{po}$  entries in Tables 7 and 8 suggests that between 16% and 20% of the pore space was open to flow for both oil and water. This result is interesting since  $F_{rrw}$  was much larger than  $F_{rro}$  at this point in the experiment (i.e.,  $F_{rrw} = 105 u^{-0.55}$  and  $F_{rro} = 14$ , from Table 4).

**Colloidal Silica.** For the colloidal-silica gel, the water-tracer studies and material balance calculations (Table 9) indicate that gel occupied about 56% of the original pore volume after three

oil-water injection cycles (86% minus 30%). Although the gel occupied a significant portion of the original pore space (56%), the permeability reductions were relatively low ( $F_{rw}=8$ ,  $F_{ro}=6$ ). No increase in residual oil saturation was observed during the second oil-water injection cycle. Table 10 shows that the oil tracer sampled only 17% of the original pore volume and the gel plus trapped water occupied 58% of the original pore volume. This means that 25% of the original pore volume was occupied by immobile oil. Thus, the gel seems to have encapsulated oil and rendered it immobile during the oil floods.

Comparing the second  $V_p/V_{po}$  entries in Tables 9 and 10 suggests that between 2% to 7% of the pore space was open to flow for both oil and water during the first water and oil injection after gel treatment. In view of these values, the residual resistance factors were surprisingly low for both oil and water ( $F_{rw}=26$ ;  $F_{ro}=23$ ).

Water- and oil-tracer curves for tracer studies before and after a gel treatment are shown in Figs. 3 and 4. In this case, the  $Cr^{3+}$ (acetate)-HPAM gel contained 1.39% HPAM and 212-ppm  $Cr^{3+}$ . Fig. 3 shows that the presence of residual oil and/or gel increased dispersivity. In contrast, the oil-tracer studies prior to gelant injection (Fig. 4) indicate that the presence of residual water had a much smaller effect on dispersivity. No significant changes in pore volume and dispersivity were observed as a result of the flow-direction reversal.<sup>16</sup> Ref. 16 contains detailed results from the tracer studies. For all of the cases studied, the presence of a residual oil saturation increased dispersivity. Also, the presence of gel increased dispersivity.

### Summary

We do not yet have a clear understanding of why some polymers and gels can reduce water permeability more than oil permeability. However, we have introduced some new tools and clues in this quest. First, before gel placement in cores, multiple imbibition and drainage cycles were performed in both flow directions. Results from these studies established that hysteresis of oil and water relative permeabilities were not responsible for the behavior observed during our subsequent gel studies. Second, several gels clearly reduced water permeability significantly more than oil permeability. Whereas previous literature reported this phenomenon for polymers and "weak" polymer-based gels, we also observed the disproportionate permeability reduction with a monomer-based gel (resorcinol-formaldehyde), as well as with both "weak"  $Cr^{3+}$ (chloride)-xanthan and "strong"  $Cr^{3+}$ (acetate)-HPAM gels. In contrast, a colloidal-silica gel reduced water and oil permeabilities by about the same factor.

Residual resistance factors for several gels were found to erode during multiple cycles of oil and water injection. In spite of this erosion, the disproportionate permeability reduction persisted through the cycles for most of the gels.

The impact of wettability on gel performance was found to vary with the gel. For a resorcinol-formaldehyde gel, the disproportionate permeability reduction was more pronounced

in Berea sandstone with an intermediate wettability than in strongly water-wet Berea sandstone. In contrast, the performance of a  $Cr^{3+}$ (chloride)-xanthan gel was less sensitive to wettability.

For  $Cr^{3+}$ (acetate)-polyacrylamide gels, an apparent shear-thinning behavior was observed during brine injection in Berea cores. For other gels, the rheology was more or less Newtonian during brine injection. For all gels investigated, the apparent rheology during oil injection was more or less Newtonian.

Studies using both oil and water tracers provided insights into the fraction of the pore volume occupied by gel. The strongest gels appeared to encapsulate the original residual oil saturation—thus rendering the residual oil inaccessible during subsequent oil flooding. For a  $Cr^{3+}$ (acetate)-polyacrylamide gel, the fraction of original pore volume that remained open to oil flow after gel placement was about the same as that for water flow (16% to 20%). However, the residual resistance factor for oil was substantially less than that for water. Also, an apparent shear-thinning behavior was observed during water injection, but Newtonian behavior was observed during oil injection.

In contrast, for a colloidal-silica gel, oil and water residual resistance factors were about the same (i.e., no disproportionate permeability reduction), and Newtonian behavior was observed during both oil and water injection. Tracer studies revealed that, during the first water and oil injection after gel treatment, the fraction of the original pore volume that remained open to flow of water or oil (2% to 4%) was significantly less than those values for the  $Cr^{3+}$ (acetate)-polyacrylamide gel. Surprisingly, the oil and water residual resistance factors were also less for the colloidal-silica gel than for the  $Cr^{3+}$ (acetate)-polyacrylamide gel. Additional research will be needed to understand these unusual findings.

### Nomenclature

- $F_{ro}$  = oil residual resistance factor (oil mobility at  $S_{wr}$  before gel placement divided by oil mobility at  $S_{wr}$  after gel placement)
- $F_{rw}$  = brine residual resistance factor (brine mobility at  $S_{or}$  before gel placement divided by brine mobility at  $S_{or}$  after gel placement)
- $k_w$  = absolute permeability to water, md [ $\mu m^2$ ]
- $k_o^o$  = end-point oil permeability, md [ $\mu m^2$ ]
- $k_w^o$  = end-point water permeability, md [ $\mu m^2$ ]
- $S_{gel}$  = gel saturation (fraction of pore volume occupied by gel)
- $S_{or}$  = irreducible oil saturation
- $S_{wr}$  = irreducible water saturation
- $u$  = superficial or Darcy velocity, ft/d [m/d]
- $V_p$  = apparent remaining pore volume,  $cm^3$
- $V_{po}$  = initial pore volume of the core,  $cm^3$
- $\alpha$  = dispersivity at the given stage in the experiment, cm
- $\alpha_o$  = initial dispersivity of the core, cm

### Acknowledgements

This work was financially supported by the U.S. Department of Energy, the New Mexico Department of Energy and Minerals, Conoco, Elf Aquitaine, Marathon Oil, Mobil Research and Development, Oryx Energy, Oxy USA, Phillips Petroleum, Shell Development, and Texaco. This support is gratefully acknowledged. The authors appreciate Yingli He's contributions in core experiments and data processing. Chromium concentrations were determined by the New Mexico BMMR Chemistry Laboratory. The authors also appreciate the help of the staff of the New Mexico Petroleum Recovery Research Center in preparing and reviewing this report.

### References

1. Liang, J., Lee, R.L., and Seright, R.S.: "Placement of Gels in Production Wells," paper SPE 20211 presented at the 1990 SPE/DOE Symposium on Enhanced Oil Recovery, Tulsa, April 22-25.
2. Seright, R.S. and Martin, F.D.: "Fluid Diversion and Sweep Improvement with Chemical Gels in Oil Recovery Processes," second annual report, Contract No. DE-FG22-89BC14447, U.S. DOE (Nov. 1991) 3-55.
3. Avery, M.R. and Wells, T.A.: "Field Evaluation of a New Gelant for Water Control in Production Wells," paper SPE 18201 presented at the 1988 SPE Annual Technical Conference and Exhibition, Houston, TX, Oct. 2-5.
4. Needham, R.B., Threlkeld, C.B., and Gall, J.W.: "Control of Water Mobility Using Polymers and Multivalent Cations," paper SPE 4747 presented at the 1974 SPE-AIME Improved Oil Recovery Symposium, Tulsa, April 22-24.
5. Sandiford, B.B. and Graham, G.A.: "Injection of Polymer Solutions in Producing Wells," AIChE Symposium Series, (1973) 69, No. 127, 38.
6. Schneider, F.N. and Owens, W.W.: "Steady-State Measurements of Relative Permeability for Polymer/Oil Systems," *SPEJ* (Feb. 1982) 79.
7. Sparlin, D.D.: "An Evaluation of Polyacrylamides for Reducing Water Production," *JPT* (Aug. 1976) 906-914.
8. White, J.L., Goddard, J.E., and Phillips, H.M.: "Use of Polymers To Control Water Production in Oil Wells," *JPT* (Feb. 1973) 143-150.
9. Zaitoun, A. and Kohler N.: "Two-Phase Flow Through Porous Media: Effect of an Adsorbed Polymer Layer," paper SPE 18085 presented at the 1988 Annual Technical Conference and Exhibition, Houston, Oct. 2-5.
10. Zaitoun, A. and Kohler N.: "Thin Polyacrylamide Gels for Water Control in High-Permeability Production Wells" paper SPE 22785 presented at the 1991 Annual Technical Conference and Exhibition, Dallas, Oct. 6-9.
11. Willhite, G.P.: *Waterflooding*, SPE, Richardson, TX (1986) 3, 21-24.
12. Jones, S.C. and Roszelle, W.O.: "Graphical Techniques for Determining Relative Permeability From Displacement Experiments," *JPT* (May 1978) 807-817.
13. Morrow, N.R., Lim, H.T., and Ward, J.S.: "Effect of Crude-Oil-Induced Wettability Changes on Oil Recovery," *SPEFE* (Feb. 1986) 89-103.
14. Jia, D., Buckley, J.S., Morrow, N.R.: "Control of Core Wettability With Crude Oil," paper SPE 21041 presented at the 1991 SPE International Symposium on Oilfield Chemistry, Anaheim, Feb. 20-22.
15. Jadhunandan, P.P.: "Effects of Brine Composition, Crude Oil, and Aging Conditions on Wettability and Oil Recovery," PhD dissertation, New Mexico Institute of Mining and Technology, Socorro, NM (1990).
16. Liang, J., Sun, H., and Seright, R.S.: "Reduction of Oil and Water Permeabilities Using Gels," New Mexico Petroleum Recovery Research Center, Socorro, NM, Report No. 91-58 (Dec. 1991).
17. Seright, R.S.: "Impact of Permeability and Lithology on Gel Performance," paper SPE 24190 presented at the 1992 SPE/DOE Symposium on Enhanced Oil Recovery, Tulsa, April 21-24.
18. Seright, R.S. and Martin, F.D.: "Impact of Gelation pH, Rock Permeability, and Lithology on the Performance of a Monomer-Based Gel," paper SPE 20999 presented at the 1991 SPE International Symposium on Oilfield Chemistry, Anaheim, Feb. 20-22.
19. Seright, R.S. and Martin, F.D.: "Effect of  $Cr^{3+}$  on the Rheology of Xanthan Formulations in Porous Media: Before and After Gelation," *In Situ* (1992) 16, No. 1.
20. Jurinak, J.J., Summers, L.E., and Bennett, K.E.: "Oilfield Application of Colloidal Silica Gel," *SPEPE* (Nov. 1991) 406-412.
21. Perkins, T.K. and Johnston, C.C.: "A Review of Diffusion and Dispersion in Porous Media," *SPEJ* (March 1963) 70-84.

Table 1. Gelant Compositions

Gelant Composition	pH
3% resorcinol, 2% formaldehyde, 0.5% KCl, 0.05M NaHCO <sub>3</sub>	6.5
0.4% xanthan, 154-ppm Cr <sup>3+</sup> (as CrCl <sub>3</sub> ), 0.5% KCl	3.8
1.39% polyacrylamide (HPAM), 636-ppm Cr <sup>3+</sup> (as acetate), 1% NaCl	6.0
1.39% HPAM, 212-ppm Cr <sup>3+</sup> (as acetate), 1% NaCl	6.0
0.7% HPAM, 318-ppm Cr <sup>3+</sup> (as acetate), 1% NaCl	6.0
10% colloidal silica, 0.7% NaCl	8.2

Table 2. Sequence Followed During Core Experiments

## Step

1. Saturate core with brine and determine porosity.
2. Determine absolute brine permeability and mobility.
3. Perform water-tracer study to confirm the pore volume ( $V_{ps}$ ) and to determine core dispersivity ( $\alpha_c$ ).
4. Inject oil (flow direction #1) to displace brine at a constant pressure drop of 100 psi across the core and determine oil mobility at residual water saturation.
5. Perform oil-tracer study (flow direction #1) to determine the fraction of the original pore volume remaining ( $V_r/V_{ps}$ ) and the relative dispersivity ( $\alpha/\alpha_c$ ).
6. Inject brine (flow direction #1) to displace oil at a constant pressure drop of 100 psi across the core and determine brine mobility at residual oil saturation.
7. Perform water-tracer study (flow direction #1) to determine  $V_r/V_{ps}$  and  $\alpha/\alpha_c$ .
8. Repeat Steps 4 through 7 (flow direction #1) to verify that the results are reproducible.
9. Reverse the flow direction (flow direction #2) and repeat Steps 4 through 7 to determine the effect of hysteresis.
10. Repeat Step 9 (flow direction #2) to verify that the results are reproducible.
11. Inject gelant using the highest possible injection rate without exceeding the pressure constraint (flow direction #1).
12. Shut in core to allow gelation.
13. Inject brine (flow direction #2) to determine the water residual resistance factors ( $F_{rw}$ ).
14. Perform water-tracer study to determine  $V_r/V_{ps}$  and  $\alpha/\alpha_c$  (flow direction #2).
- 15a. Inject oil (flow direction #2) to determine the oil residual resistance factor ( $F_{ro}$ ).
- 15b. Perform oil-tracer study to determine  $V_r/V_{ps}$  and  $\alpha/\alpha_c$  (flow direction #2).
- 15c. Inject brine (flow direction #2) to determine  $F_{rw}$ .
- 15d. Perform water-tracer study to determine  $V_r/V_{ps}$  and  $\alpha/\alpha_c$  (flow direction #2).
16. Repeat Steps 15a through 15d (second oil-water injection cycle after shut-in).
17. Repeat Steps 15a through 15d (third oil-water injection cycle after shut-in).

\* 30 psi if gelant was resorcinol-formaldehyde.

Table 3. Effect of Flow-Direction Reversal on End-Point Permeabilities (41°C)

Core ID	Wettability	$k_s$ , md	$k_s^*$ , md	$k_o$ , md	$k_o^*$ , md
SSH-17	Strongly water-wet	718	719	182	169
SSH-22	Strongly water-wet	706	792	186	206
SSH-26	Strongly water-wet	593	594	177	170
SSH-15	Intermediate	1680	1413	151	261
SSH-23	Intermediate	891	909	277	402

\* Flow-direction reversed.

Table 4. Summary of Residual Resistance Factors for Brine ( $F_{rw}$ ) and Oil ( $F_{ro}$ )

Core ID	Wettability	Gel Type	$F_{rw}$ (Step 13)	$F_{ro}$ (Step 15a)	$F_{rw}$ (Step 15c)	$F_{ro}$ (Step 16a)	$F_{rw}$ (Step 16c)	$F_{ro}$ (Step 17a)	$F_{rw}$ (Step 17c)
SSH-17	Strongly water-wet	resorcinol-formaldehyde	49	11	40	12	41	--	--
SSH-15	Intermediate	resorcinol-formaldehyde	510	26	180	29	241	--	--
SSH-22	Strongly water-wet	Cr <sup>3+</sup> (chloride)-xanthan	8	5	12	4	8	--	--
SSH-23	Intermediate	Cr <sup>3+</sup> (chloride)-xanthan	22	14	31	16	42	--	--
SSH-26	Strongly water-wet	1.39% HPAM, 636-ppm Cr <sup>3+</sup>	40,000	1,020	12,314	148	2,175	100	409 u <sup>-0.45</sup>
SSH-27	Strongly water-wet	0.7% HPAM, 318-ppm Cr <sup>3+</sup>	829 u <sup>-0.45</sup>	20	117 u <sup>-0.29</sup>	15	33 u <sup>-0.33</sup>	--	--
SSH-31	Strongly water-wet	1.39% HPAM, 212-ppm Cr <sup>3+</sup>	52,954	50	972 u <sup>-0.30</sup>	25	357 u <sup>-0.40</sup>	14	105 u <sup>-0.35</sup>
SSH-32	Strongly water-wet	colloidal silica	26	23	14	9	12	6	8

u is superficial velocity (in ft/d)

Table 5. Pore Volume Determinations from Water-Tracer Studies, Core SSH-17 (Oil Phase: Soltrol-130, Gelant: Resorcinol-Formaldehyde)

Tracer Study	$V_r/V_p$	$1-V_r/V_p$	$S_w$
After 1st waterflood (Step 7)*	0.72	0.28	0.28
After 2nd waterflood (Step 8)	0.72	0.28	0.29
After 3rd waterflood (Step 9)	0.69	0.31	0.32
After 4th waterflood (Step 10)	0.69	0.31	0.34
1st waterflood after gel treatment (Step 14)	0.63	0.37	0.34
2nd waterflood after gel treatment (Step 15d)	0.38	0.62	--

\* All steps in this table and subsequent tables are described in Table 2.

Table 6. Pore Volume Determinations from Water-Tracer Studies, Core SSH-22 (Oil Phase: Soltrol-130, Gelant: Cr<sup>3+</sup>(chloride)-Xanthan)

Tracer Study	$V_r/V_p$	$1-V_r/V_p$	$S_w$
After 1st waterflood (Step 7)	0.68	0.32	0.31
After 2nd waterflood (Step 8)	0.67	0.33	0.34
After 3rd waterflood (Step 9)	0.65	0.35	0.33
After 4th waterflood (Step 10)	0.67	0.33	0.33
1st waterflood after gel treatment (Step 14)	0.39	0.61	0.33
2nd waterflood after gel treatment (Step 15d)	0.20	0.80	--
3rd waterflood after gel treatment (Step 16d)	0.19	0.81	--

Table 7. Pore Volume Determinations from Water-Tracer Studies,  
Core SSH-31 (Oil Phase: Soltrol-130, Gelant:  $\text{Cr}^{2+}$ (acetate)-HPAM; 1.39% HPAM, 212-ppm  $\text{Cr}^{2+}$ )

Tracer Study	$V_p/V_{ps}$	$1-V_p/V_{ps}$	$S_w$
After 1st waterflood (Step 7)	0.72	0.28	0.29
1st waterflood after gel treatment (Step 14)	--	--	0.29
2nd waterflood after gel treatment (Step 15d)	--	--	0.34
3rd waterflood after gel treatment (Step 16d)	0.15	0.85	0.33
4th waterflood after gel treatment (Step 17d)	0.16	0.84	0.33

Table 8. Pore Volume Determinations from Oil-Tracer Studies,  
Core SSH-31 (Oil phase: Soltrol-130, Gelant:  $\text{Cr}^{2+}$ (acetate)-HPAM; 1.39% HPAM, 212-ppm  $\text{Cr}^{2+}$ )

Tracer Study	$V_p/V_{ps}$	$1-V_p/V_{ps}$	$S_w$
After 1st oilflood (Step 5)	0.72	0.28	0.29
1st oilflood after gel treatment (Step 15b)	0.12	0.88	0.59*
2nd oilflood after gel treatment (Step 16b)	0.14	0.86	0.57*
3rd oilflood after gel treatment (Step 17b)	0.20	0.80	0.55*

\*  $S_w + S_{gel}$

Table 9. Pore Volume Determinations from Water-Tracer Studies,  
Core SSH-32 (Oil Phase: Soltrol-130, Gelant: Colloidal Silica)

Tracer Study	$V_p/V_{ps}$	$1-V_p/V_{ps}$	$S_w$
After 1st waterflood (Step 7)	0.72	0.28	0.28
1st waterflood after gel treatment (Step 14)	0.02	0.98	0.28
2nd waterflood after gel treatment (Step 15d)	0.07	0.93	0.29
3rd waterflood after gel treatment (Step 16d)	0.14	0.86	0.28
4th waterflood after gel treatment (Step 17d)	0.14	0.86	0.30

Table 10. Pore Volume Determinations from Oil-Tracer Studies,  
Core SSH-32 (Oil Phase: Soltrol-130, Gelant: Colloidal Silica)

Tracer Study	$V_p/V_{ps}$	$1-V_p/V_{ps}$	$S_w$
After 1st oilflood (Step 5)	0.75	0.25	0.26
1st oilflood after gel treatment (Step 15b)	0.04	0.96	0.61*
2nd oilflood after gel treatment (Step 16b)	0.13	0.87	0.61*
3rd oilflood after gel treatment (Step 17b)	0.17	0.83	0.58*

\*  $S_w + S_{gel}$

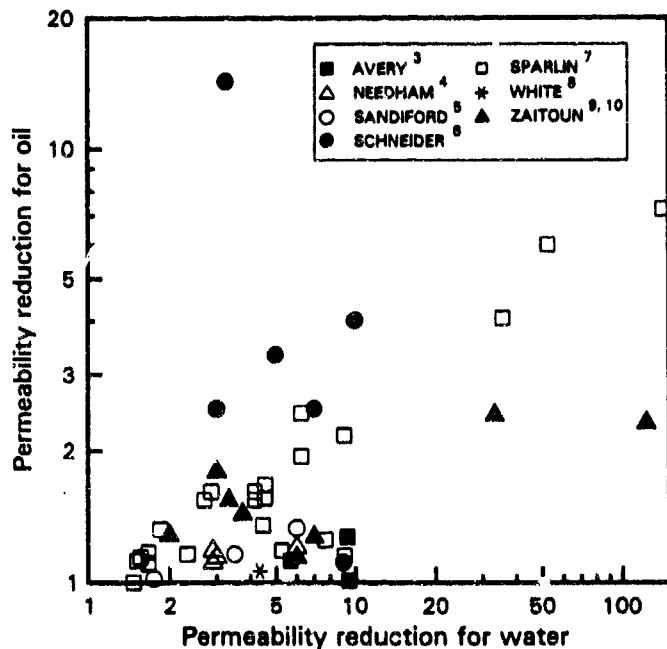


Fig. 1. Disproportionate permeability reduction by polymers and gels.

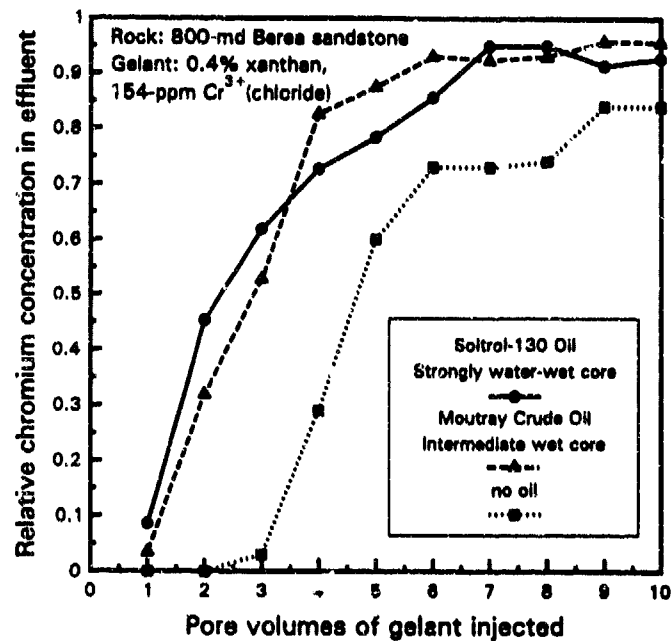


Fig. 2. Chromium propagation through porous media.

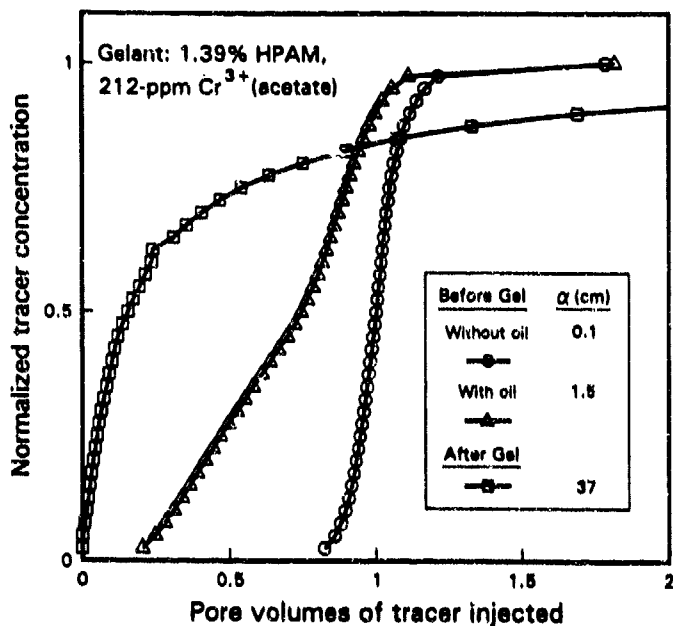


Fig. 3. Effects of the presence of residual oil and gel on dispersivities from water tracer studies.

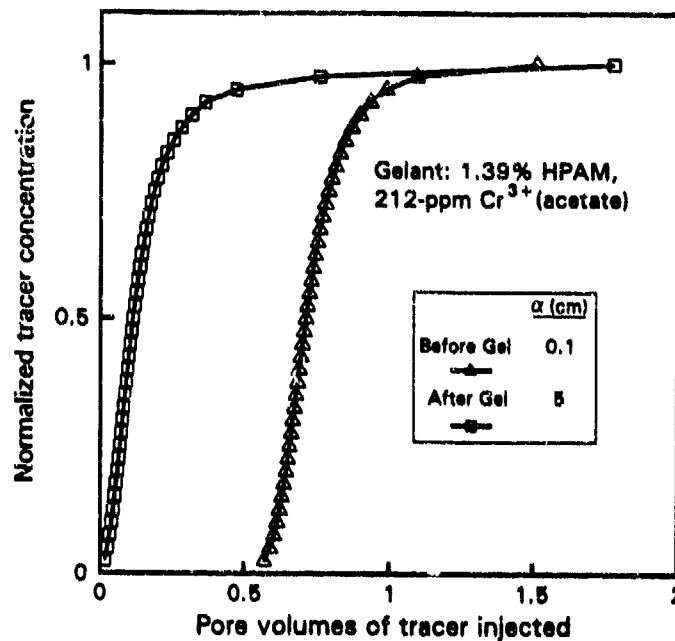


Fig. 4. Effects of the presence of residual water and gel on dispersivities from oil tracer studies.